Quasiparticle Screening near a Bosonic Superconductor-Insulator Transition Revealed by Magnetic Impurity Doping

Xue Zhang, James C. Joy, Chunshu Wu, Jin Ho Kim, J. M. Xu, and James M. Valles, Jr.

Phys. Rev. Lett. **122**, 157002 — Published 19 April 2019

DOI: 10.1103/PhysRevLett.122.157002

Quasiparticle Screening near a Bosonic Superconductor-Insulator Transition Revealed by Magnetic Impurity Doping

Xue Zhang,[1] James C. Joy,[1] Chunshu Wu,[1] Jin Ho Kim,[2] J. M. Xu,[2] and James M. Valles, Jr.[1]

[1]*Department of Physics, Brown University, Providence, RI, USA*
[2]*School of Engineering, Brown University, Providence, RI, USA*

Experiments show that the Cooper pair transport in the insulator phase that forms at thin film superconductor to insulator transitions (SIT) is simply activated. The activation energy T_0 depends on the microscopic factors that drive Cooper pair localization. To test proposed models, we investigated how a perturbation that weakens Cooper pair binding, magnetic impurity doping, and phase frustration affects T_0. The data show that T_0 decreases monotonically with doping in films tuned farther from the SIT and increases and peaks in films that are closer to the SIT critical point. The observations provide strong evidence that the bosonic SIT in thin films is a Mott transition driven by Coulomb interactions that are screened by virtual quasi-particle excitations. This dependence on underlying fermionic degrees of freedom distinguishes these SITs from those in micro-fabricated Josephson Junction Arrays, cold atom systems, and likely in high temperature superconductors with nodes in their quasiparticle density of states.

What drives Cooper pair localization in films undergoing a superconductor-insulator quantum phase transition (SIT) has not been resolved[1]. In some models[2–4] the localization arises mainly from disorder induced Anderson localization effects[5] and in others from repulsive Coulomb interaction or Mott transition effects[6–8]. Experiments have been unable to discern the primary driver despite having established myriad signature characteristics of the Cooper pair insulator state like its giant positive magnetoresistance[9–12], islanded structure[13,14] and Cooper pair dominated transport[15,16]. Here, we present magnetic impurity doping studies, which reveal that Coulomb interaction effects dominate the superconductor-Cooper pair insulator transition in a-Bi thin films.

These investigations focus on the activation energy, T_0, determined from the temperature dependence of the sheet resistance of the Cooper pair insulator

$$R(T) = R_0 \exp(T_0/T) \tag{1}$$

where R_0 is a constant and T is the temperature[9,17,18]. Motivation for this focus is that the activation energy in a condensed matter system offers a window into its quantum many body ground state. For example, T_0 of a fractional quantum hall liquid is the energy required to create spatially separated quasiparticle-quasihole pairs out of the Laughlin ground state[19–21]. Similarly, the low temperature heat capacity of conventional superconductors is characterized by an activation energy corresponding to half the binding energy, 2Δ, of electrons in Cooper pairs in the BCS ground state[22]. At this point it is known that T_0 for the Cooper pair insulator controls the rate of Cooper pair tunneling between localized states[15] but differs from the Cooper pair binding energy since it grows from zero at the SIT critical point where $\Delta \neq 0$[15].

In models of the Cooper pair insulator, T_0 results from a competition between pair tunneling, characterized by a hopping rate t or a Josephson coupling energy, E_J, that delocalizes pairs and either potential disorder or Coulomb interactions that localize pairs. Potential disorder drives Anderson localization[2,3,23] of pair states with energies below a mobility edge in the density of states. T_0 corresponds to the gap between localized and mobile pair states[3,24,25] and increases with disorder or decreasing t. Coulomb interactions, on the other hand, drive a Mott transition by creating a blockade to pair motion between localized states[26]. The blockade is characterized by a charging energy, $E_c = 2e^2/C$, that depends on the capacitance between a localized state and its environment[7,8,26–29]. In the limit, $E_c \gg E_J$, a Mott gap appears in the transport,

$$T_0 \approx E_c \left(1 - \frac{z}{2}\frac{E_J}{E_c}\right) \tag{2}$$

with a second term that depends on coordination number z and E_J to account for Cooper pair screening[7,30]. Measuring how T_0 responds to changes in parameters like E_J is necessary to test these models of Cooper pair localization. While previous experiments showed that T_0 depends on many factors including magnetic field[9,12,18,31], magnetic frustration[32] and normal state resistance[10,33], the relations between the factors and model parameters have not been defined well enough to compare directly with models.

We have employed a thin film platform[15] that enables unique methods for probing the origins of T_0. The films can be systematically doped with magnetic impurities, which reduces 2Δ and can be subjected to magnetic frustration, which reduces the average Josephson coupling between localized regions[12] (see Figs. 1 a,b). Since $E_J \propto \Delta$, the doping also reduces E_J. For both the Anderson and Mott classes of models, reducing E_J is expected to enhance T_0 and thus, Cooper pair localization. Surprisingly, we found that while magnetic frustration always enhances T_0, magnetic impurity doping can reduce T_0. We discuss how this result intimates that the superconductor to Cooper pair insulator transition is a Mott transition with a Coulomb blockade energy that depends

on the pair binding energy.

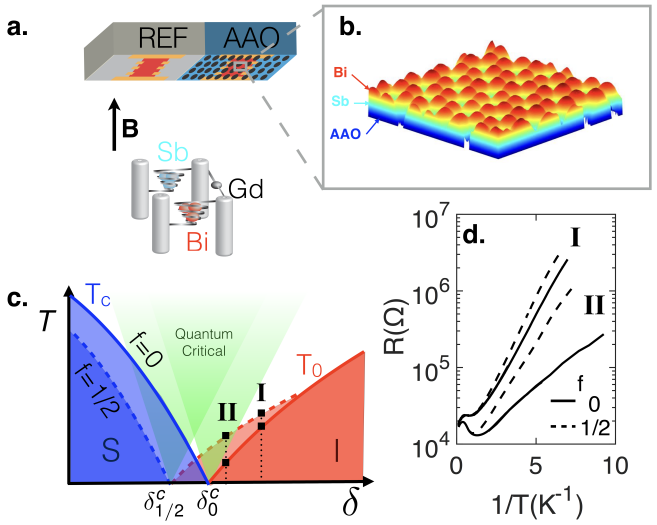

FIG. 1. a) Sketch of experimental set-up displaying side by side flat glass (REF) and AAO substrates positioned over the Sb, Bi, and Gd evaporation sources in a magnetic field **B** directed as shown. b) Atomic force microscopy (AFM) image of AAO falsely colored to indicate the evaporation layers, substrate height variations and 100 nm period nanopore array. c) Schematic phase diagram of temperature vs. coupling constant, $\delta \sim R_N$ for a superconductor to Cooper Pair Insulator quantum phase transition. I and II refer to the films investigated. There is a critical point for each of the frustrations, $f = 0$ and $1/2$. d) Sheet resistance on a logarithmic scale versus inverse temperature for undoped films, I and II, at $f = 0$ (solid lines) and $f = 1/2$ (dashed lines).

Sub-nanometer thick amorphous Bi films were fabricated and measured *in situ* in the UHV environment of a dilution refrigerator based evaporator. Bi vapor was quench condensed onto an Sb wetting layer on the surface of two substrates simultaneously: an Anodized Aluminum Oxide substrate, which has regular height variations and an array of pores, and a flat, fire polished glass substrate. Both substrates were held at a temperature, $T = T_s \approx 10$ K within the UHV environment of a dilution refrigerator cryostat (Fig. 1). The depositions of Bi and Sb were measured using a quartz crystal micro-balance.

The Cooper pair insulator state forms in films on AAO substrates because of nanometer scale height variations, $h(x)$ on the AAO surface (see Fig. 1b)[33]. Surrounding most pores there are 6 peaks. The surface slope variations around each pore produces film thickness variations $d(x)$:

$$d(x) = \frac{d^{\rm dep}}{\sqrt{1 + (\nabla h(x))^2}} \qquad (3)$$

The 6 peaks thus give rise to 12 dots of thicker film in the peaks and valleys. Since T_c increases with film thickness[34] these dots form an array of sites that localize Cooper pairs in insulating films. Insulating films on flat substrates, by contrast, have only weakly localized, unpaired electrons[3536,37]. The film on the flat substrate served as a reference for monitoring 1) the maximum thickness and pairing amplitude that could appear in the films deposited on AAO and 2) the pair breaking effects of the magnetic impurity depositions.

Film sheet resistances were measured as a function of temperature, $R(T)$ *in situ* using standard four-point ac and dc techniques with sufficiently low current bias(0.2 nA) to ensure that the measurements were performed in the linear portion of the current-voltage characteristics. A superconducting solenoid applied magnetic fields perpendicular to the films.

The array of pores in the films enable us to explore magnetic field induced frustration effects on the Cooper pair insulator phase. The appearance of oscillations in the magnetoresistance was an early direct sign of localized Cooper pairs in a thin film system[15]. The activation energy and location of the SIT critical point (see Fig. 1 c) is periodic in the frustration $f = H/H_M$, where H_M is the magnetic field that produces one superconducting flux quantum per plaquette. $H_M = 0.21T$ for the 100 nm average center to center spacing of nearest neighbor pores. This frustration dependence can be attributed to a modulation of the average Josephson coupling between islands with a period of one flux quantum per plaquette[12,38]. The average appears as $< E_J >= E_{J0} < \sum_{<i,j>} \cos(\phi_i - \phi_j - A_{ij}) >$ where ϕ_i and ϕ_j are the phases on neighboring islands and A_{ij} is the line integral of the vector potential between islands. For a honeycomb array of islands, the energy barrier for Cooper pair transport is highest for $f = 1/2$[39]. Phenomenologically, $< E_J(f) > \propto E_{J0}F(2\pi f)$, where F is a periodic function with maxima of 1 at integer f.

Magnetic impurity doping involved depositing Gd atop the Cooper pair insulator film[40]. The impurities produce time reversal symmetry breaking spin flip scattering, which reduces the pair binding energy 2Δ. Their effect extends uniformly through the entire thickness of the films since the films are much thinner ($d \leq 1$ nm) than the superconducting coherence length ($\xi \geq 10$ nm)[41]. The Gd deposition amounts, x_{Gd}, which were below the micro-balance resolution, were monitored using a calibrated timing method and by measuring their effects on the T_c of the reference film. The two methods agreed well. In the following, the relative T_c shift on the reference film

$$\alpha_{Gd} = 1 - T_c(x_{Gd})/T_c(0) \qquad (4)$$

to represent the pair breaking strength. The estimated maximum Gd doping in these experiments corresponded to < 0.03 monolayers.

We studied the effects of magnetic impurity doping and magnetic frustration on two films, I and II, that had different activation energies to explore how proximity to the SIT critical point influences the response. Points for films I and II are indicated on the schematic phase diagram in Fig. 1c. according to their relative activation

TABLE I. Film I and II parameters.

	R_N	d_{Bi}	$T_0(0)$	$T_0(1/2)$	$T_c(0)$
I	18.6 $k\Omega$	0.99 nm	0.86 K	0.98 K	2.59 K
II	16.7 $k\Omega$	1.2 nm	0.40 K	0.75 K	2.92 K

energies obtained from fits to the data shown in Fig. 1d. Other film I and II parameters are in the Table. The phase diagram shows two distinct critical points for the two frustrations investigated, $f = 0$ and $f = 1/2$[42]. The tuning parameter δ, corresponds to either $1/d$ or R_N, where R_N is sheet resistance measured at 8K. Previous work[15] indicated that the critical values of the tuning parameters for the SIT followed $\delta_0^c > \delta_{1/2}^c$.

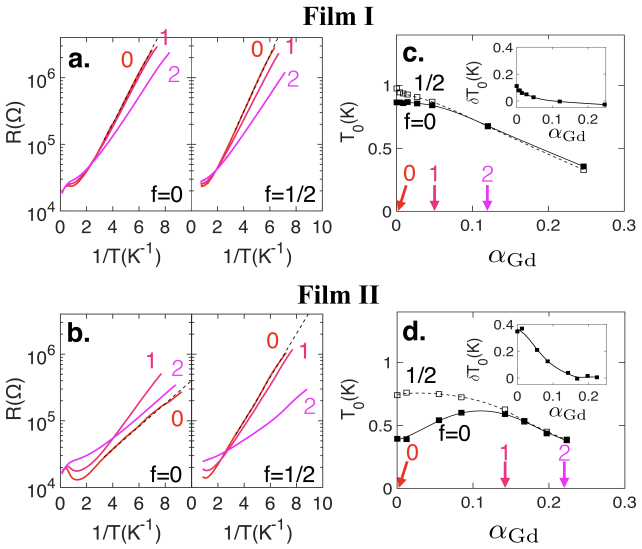

FIG. 2. Magnetic Impurity Doping Response of Resistance and Activation Energy. Left panels: Arrehenius plots of $R(T)$ at 3 Gd doping levels for both $f = 0$ and $f = 1/2$ for films I (a) and II (b). The numerical labels increase with Gd doping, where 0 represents no doping. The dashed lines give examples of linear fits that yield T_0 values. Right panels: Activation energy vs. pairbreaking strength for films I (c) and II (d). The arrows indicate the pairbreaking strengths corresponding to $R(T)$ in the left panels. The filled squares correspond to $f = 0$ and open squares are $f = 1/2$. The lines are guides to the eye. Insert: $\delta T_0 = T_0^{f=1/2} - T_0^{f=0}$ as a function of doping induced pairbreaking.

The effects of Gd doping on films I and II at the two frustrations $f = 0$ and $f = 1/2$ are displayed in Fig. 2. The Arrhenius plots show that their $R(T)$ are activated through the doping range. The evolution of $T_0(f, \alpha_{Gd})$ with doping depends on its undoped value, $T_0(f, 0)$. For the three cases with the largest $T_0(f, 0)$, T_0 decreases or remains nearly constant at low doping and then decreases. By contrast, the film with the lowest $T_0(f, 0)$ exhibits a maximum in T_0. The difference between the activation energies at the two frustrations, $\delta T_0 = T_0(1/2) - T_0(0)$, is larger for the film closer to the SIT. For both films, δT_0 goes to zero, nearly linearly, at higher doping levels.

The response of T_0 to frustration can be accounted for by all of the discussed models. For both films at low fields $\delta T_0 = T_0(1/2) - T_0(0) \neq 0$ indicating that Cooper pair transport dominates[15]. More importantly, the increase in T_0 with frustration (i.e. f=1/2) is consistent with frustration reducing $< E_J >$. This reduction increases the mobility gap[3] or reduces the Cooper pair screening of the Coulomb blockade energy to increase T_0[7,30]. The fact that $T_0(1/2) - T_0(0)$ is larger for film II, which is closer to the SIT, shows that the frustration effect grows with the interisland tunneling rate.

By contrast, T_0's doping dependence does not align with simple expectations for three cases (film I at f=0 and f=1/2, and film II at f=1/2). Pairbreaking reduces 2Δ, which should reduce E_J or t to make T_0 rise. Similarly if the impurities were to randomly transform links into π junctions[43], their effect would be to reduce E_J or t to make T_0 rise at large doping[44]. Thus, these three cases rule out disorder induced localization models in which t is the only Δ dependent parameter[3]. They also rule out Coulomb interaction models in which E_c depends only on the geometry of the localized states and the local dielectric constants[8]. Magnetic impurity doping is not expected to influence dielectric properties. It might influence the geometry by causing the islands to shrink. That effect, however, would increase charging energies and thus, T_0.

A possible explanation for T_0 decreasing with pairbreaking is that E_c depends directly on Δ. This dependence emerges when the inter island charging energy greatly exceeds the pair binding energy Δ, i.e. $E_c \gg \Delta$[7,45–47]. In this limit, virtual quasiparticle tunneling processes, which depend on Δ, renormalize the capacitance of single junctions[46,47]. An estimate of E_c for the dots in the a-Bi films indicates they are in this limit. For 12 equivalent dots to fit around each pore, the dot radii must be $r_{dot} = 13nm$. Using this length scale and the dielectric constant of aluminum oxide $\epsilon = 10$ gives $E_c \approx \epsilon\epsilon_0 r_{dot}/k_B \approx 3000K \gg \Delta$. Beloborodov and coworkers[7] included this effect in a model of granular films to derive a renormalized charging energy:

$$\tilde{E}_c = \frac{2\Delta}{3\pi^2 g} \ln\left(gE_{c0}/\Delta\right) \qquad (5)$$

where $g = G/(2e^2/\hbar)$ is the dimensionless normal state conductance between grains and E_{c0} is the self charging energy of a dot. Thus, the charging energy becomes Δ dependent.

Using $\tilde{E}_c$ in Eq.(2), yields:

$$T_0 = \frac{2\Delta}{3\pi^2 g} \ln\left(gE_{C0}/\Delta\right) - \frac{zg\Delta}{2} F(2\pi f) \qquad (6)$$

which can be compared with the experimental results (see Fig. (3)) using parameters, Δ, z, E_{c0}, and g, fixed by measurements. Taking the temperature at which the

reference film resistance drops to 10 % of its normal state resistance as T_{c0}, gives $\Delta(\alpha_{Gd}=0) = 1.7k_BT_{c0}$ presuming the weakly coupled BCS relation between Δ and T_{c0} as appropriate for a-Bi films near the SIT[36]. The result is insensitive to the specific choice of the 10% criterion because of the 5% width of the resistance transitions and relatively weak dependence of T_0 on variations in T_{c0}. With pairbreaking, the minimum energy for excitations becomes the spectral gap Ω_G, rather than Δ, the pairing potential. Thus, the calculated evolution of the spectral gap $\Omega_G(\alpha_{Gd})$ with doping[48] is used instead of $\Delta(\alpha_{Gd})$. $z = 2.5$ is the average coordination for the dot arrays since half the islands have $z = 2$ and half have $z = 3$. E_{c0} is determined presuming the Josephson Junction array model[7] employed to get Eq. (2). The dots are treated as disks on the surface of aluminum oxide in vacuum so that $E_{c0} = 4e^2/(8\epsilon\epsilon_0 r_{dot})$ with $\epsilon = 10$ and $r_{dot} = 13nm$ as estimated above. The interisland conductances, g are set by the normal state sheet resistance as $g = 3\frac{\hbar}{2e^2}/R_N$[33]. The expression for T_0, however, is sensitive to variations in g that are smaller than the $\approx 10\%$ systematic uncertainties in measuring R_N. Consequently, the g's were set within the window of uncertainty using $R_N = 18.9k\Omega$ and 17.6Ω to make the calculated T_0's at zero doping coincide with the data, for films I and II, respectively. Finally, $F(0) = 1$ and the $F(1/2)$ values were set in accord with predictions of a theory of the magneto resistance oscillations[49]. That theory indicates that $F(1/2)$ grows from 0.9 and 1.0 with increasing distance from the SIT. Accordingly, $F(1/2)$ was set to 0.96 and 0.905 for films I and II, respectively, to match the zero doping data points in Fig. (3).

The predictions of Eq. (6) compare well with the data (see Fig. 3). Qualitatively, the calculated and measured T_0 decrease monotonically with doping for films with lower g that are farther from the SIT and develop a maximum at higher g. Quantitatively, the predicted and measured variations in T_0 are similar in size. The α_{Gd} scales for the data and the calculation differ by about a factor of two. This difference could indicate that the spectral gap to T_{c0} ratio decreases more rapidly in nanodots than predicted for bulk materials. Altogether, the agreement implies that 1) these Cooper pair insulators are Mott insulators with screened Coulomb interactions and 2) the non-monotonic behavior of $T_0(\alpha_{Gd})$ reflects the different Δ dependencies of the first term ($\propto \Delta \log \Delta$) and the second term ($\propto \Delta$) in Eq. 6.

This Mott phase is distinct. The screening effect differentiates it from the unscreened Mott transition observed in micro-fabricated Josephson Junction Arrays for which $\Delta > E_c$[50]. Similarly, it differs from cold atom system Mott transitions, which have short range interactions and bosons that cannot decompose into constituent parts[51].It is interesting also to consider implications for bosonic SITs in high temperature superconducting cuprates[52]. The nodes in their d-wave density of states could make virtual quasiparticle screening more effective than in fully gapped s-wave systems. Smaller T_0's and/or deviations from simply activated transport could arise.

Finally, the disappearance of T_0's frustration dependence at higher doping levels likely signals a crossover from transport that involves Cooper pairs to quasiparticle dominated transport. The crossover is smooth: the $R(T)$ (Figs. 2a,b) maintain an activated form and T_0 evolves without any clear discontinuities in its value or slope. The continued decrease of T_0 with Gd doping suggests that the quasi-particle transport depends directly on the Cooper pair binding energy. This dependence arises for quasi-particle tunneling between superconducting dots as proposed to explain negative magnetoresistance in granular Pb[53] and Indium Oxide films[54]. Within this model, the inferred values of 2Δ at the crossover, presuming $T_0 = 2\Delta$, are 0.83 K and 0.6 K for films I and II, respectively. Both of these values fall below the transition temperatures of their associated reference films, which makes them reasonable.

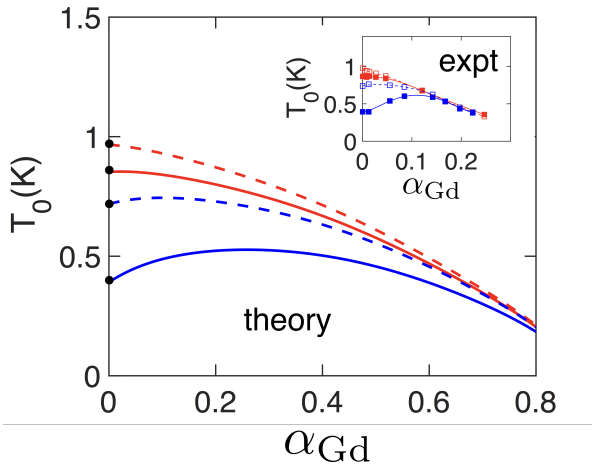

FIG. 3. Comparison with Mott Insulator Transport Model with Virtual Quasiparticle Screening. Activation energy as a function of magnetic impurity doping calculated using Eq. 6 as described in the text. The red and blue lines correspond to films I and II, respectively and the solid and dashed lines correspond to $f = 0$ and $f = 1/2$, respectively. The black dots give the measured T_0 at zero doping. Inset: Representation of the experimental results in Fig. 2 for films I and II with lines to guide the eye.

To summarize, we investigated the influence of magnetic impurity doping, magnetic frustration, and sheet resistance on the transport activation energy, T_0, of the Cooper pair insulator phase in amorphous Bi films on AAO substrates. T_0's response implies that it depends directly on the energy binding the Cooper pairs and agrees well with a model[7] of the Cooper Pair Insulator as a Mott Insulator in which virtual quasi-particle tunneling processes screen the Coulomb interactions that impede boson tunneling transport. The results rule out a number of other models[2–4,6,8] and distinguish this Cooper pair insulator phase from that in micro-fabricated Josephson Junction arrays[50] and the bose insulator phase in cold

atom systems[51] in which virtual quasiparticle processes exert negligible influence.

ACKNOWLEDGEMENTS

We are grateful to S. Kivelson, N. Trivedi, M. Mueller, and especially, I. Beloborodov and E. Granato for helpful discussions. This work was partially supported by NSF Grant Nos. DMR-1307290 and DMR-1408743 and the AFOSR.

[1] V. F. Gantmakher and V. T. Dolgopolov, Physics-Uspekhi **53**, 1 (2010).
[2] K. Bouadim, Y. L. Loh, M. Randeria, and N. Trivedi, Nature Physics **7**, 884 (2011).
[3] A. Gangopadhyay, V. Galitski, and M. Muller, Physical Review Letters **111**, 026801 (2013).
[4] Y. L. Loh, M. Randeria, N. Trivedi, C. C. Chang, and R. Scalettar, Physical Review X **6**, 021029 (2016), arXiv:1507.05641.
[5] V. Dobrosavljevic, N. Trivedi, and J. M. Valles Jr, *Conductor Insulator Quantum Phase Transitions*, Vol. 16 (Oxford University Press, 2012).
[6] Y. Dubi, Y. Meir, and Y. Avishai, Physical Review B **73**, 054509 (2006).
[7] I. S. Beloborodov, A. V. Lopatin, V. M. Vinokur, and K. B. Efetov, Reviews of Modern Physics **79**, 469 (2007), arXiv:0603522 [cond-mat].
[8] M. V. Fistul, V. M. Vinokur, and T. I. Baturina, Physical Review Letters **100**, 086805 (2008).
[9] G. Sambandamurthy, L. W. Engel, A. Johansson, and D. Shahar, Physical Review Letters **92**, 107005 (2004), arXiv:0307648 [cond-mat].
[10] M. Steiner and A. Kapitulnik, Physica C-Superconductivity and Its Applications **422**, 16 (2005).
[11] T. I. Baturina, A. Y. Mironov, V. M. Vinokur, M. R. Baklanov, and C. Strunk, Physical Review Letters **99**, 257003 (2007).
[12] H. Q. Nguyen, S. M. Hollen, M. D. Stewart, J. Shainline, A. Yin, J. M. Xu, and J. M. Valles, Physical Review Letters **103**, 157001 (2009), arXiv:0907.4120v2.
[13] B. Sacepe, C. Chapelier, T. I. Baturina, V. M. Vinokur, M. R. Baklanov, and M. Sanquer, Physical Review Letters **101**, 157006 (2008).
[14] B. Sacepe, T. Dubouchet, C. Chapelier, M. Sanquer, M. Ovadia, D. Shahar, M. Feigel'man, and L. Ioffe, Nature Physics **7**, 239 (2011).
[15] M. D. Stewart, A. Yin, J. M. Xu, and J. M. Valles, Science **318**, 1273 (2007).
[16] G. Kopnov, O. Cohen, M. Ovadia, K. H. Lee, C. C. Wong, and D. Shahar, Physical Review Letters **109**, 167002 (2012).
[17] T. I. Baturina, A. Y. Mironov, V. M. Vinokur, M. R. Baklanov, and C. Strunk, Jetp Letters **88**, 752 (2008), arXiv:0810.4351.
[18] Y.-H. H. Lin, J. Nelson, and A. M. Goldman, Physica C-Superconductivity and Its Applications **497**, 102 (2014).
[19] R. B. Laughlin, Physical Review Letters **50**, 1395 (1983), arXiv:1111.4781.
[20] G. S. Boebinger, H. L. Stormer, D. C. Tsui, A. M. Chang, J. C. M. Hwang, A. Y. Cho, C. W. Tu, and G. Weimann, Phys. Rev. B **36**, 7919 (1987).
[21] S. M. Girvin, A. H. MacDonald, and P. M. Platzman, Physical Review Letters **54**, 581 (1985).
[22] M. Tinkham, The McGraw-Hill Companies, Inc. (1996).
[23] M. V. Feigel'man, L. B. Ioffe, V. E. Kravtsov, and E. Cuevas, Annals of Physics **325**, 1390 (2010), arXiv:1002.0859.
[24] S. V. Syzranov, K. B. Efetov, and B. L. Altshuler, Physical Review Letters **103**, 127001 (2009).
[25] T. T. Nguyen and M. Müller, , 1 (2016), arXiv:1606.07747.
[26] K. B. Efetov, Sov. Phys. JETP **51**, 1015 (1980).
[27] M. C. Cha and S. M. Girvin, Physical Review B **49**, 9794 (1994).
[28] T. I. Baturina and V. M. Vinokur, Annals of Physics **331**, 236 (2013).
[29] M. Swanson, Y. L. Loh, M. Randeria, and N. Trivedi, Physical Review X **4**, 021007 (2014).
[30] R. Fazio and G. Schön, Physical Review B **43**, 5307 (1991).
[31] T. I. Baturina, C. Strunk, M. R. Baklanov, and A. Satta, Physical Review Letters **98**, 127003 (2007).
[32] M. D. Stewart, A. Yin, J. M. Xu, and J. M. Valles, Physical Review B **77**, 140501(R) (2008).
[33] S. M. Hollen, H. Q. Nguyen, E. Rudisaile, M. D. Stewart, J. Shainline, J. M. Xu, and J. M. Valles, Physical Review B **84**, 064528 (2011).
[34] J. M. Valles, A. E. White, K. T. Short, R. C. Dynes, J. P. Garno, A. F. J. Levi, M. Anzlowar, and K. Baldwin, Physical Review B **39**, 11599 (1989).
[35] A. M. Finkelstein, Physica B-Condensed Matter **197**, 636 (1994).
[36] J. M. Valles Jr., R. C. Dynes, and J. P. Garno, Phys. Rev. Lett. **69**, 3567 (1992).
[37] S. M. Hollen, G. E. Fernandes, J. M. Xu, and J. M. Valles, Physical Review B **87**, 054512 (2013), arXiv:1301.6155.
[38] M. Müller, EPL (Europhysics Letters) **102**, 67008 (2013).
[39] E. Granato, European Physical Journal B **89**, 1 (2016), arXiv:1602.04509v1.
[40] J. S. Parker, D. E. Read, A. Kumar, and P. Xiong, Europhysics Letters **75**, 950 (2006).
[41] J. A. Chervenak and J. M. Valles, Physical Review B **51**, 11977 (1995).
[42] E. Granato, Physica B: Condensed Matter **536**, 442 (2018).
[43] L. N. Bulaevskii, V. V. Kuzii, and A. A. Sobyanin, JETP Letters **25**, 290 (1977).
[44] E. Granato, Physical Review B **96**, 184510 (2017).
[45] A. I. Larkin and Y. N. Ovchinnikov, Physical Review B **28**, 6281 (1983).
[46] V. Ambegaokar, U. Eckern, and G. Schön, Physical Review Letters **48**, 1745 (1982).

[47] S. Chakravarty, S. Kivelson, G. T. Zimanyi, and B. I. Halperin, Physical Review B **35**, 7256 (1987).
[48] S. Skalski, O. Betbeder-Matibet, and P. R. Weiss, Physical Review **136**, A1500 (1964).
[49] T. T. Nguyen and M. Müller, , 1 (2016), arXiv:1606.07747.
[50] P. Delsing, C. D. Chen, D. B. Haviland, Y. Harada, and T. Claeson, Physical Review B **50**, 3959 (1994).
[51] M. Greiner, O. Mandel, T. Esslinger, T. W. Hänsch, and I. Bloch, Nature **415**, 39 (2002).
[52] A. T. Bollinger, G. Dubuis, J. Yoon, D. Pavuna, J. Misewich, and I. Bozovic, Nature **472**, 458 (2011).
[53] R. P. Barber, S.-Y. Hsu, J. M. Valles, R. C. Dynes, and R. E. Glover, Physical Review B **73**, 134516 (2006).
[54] V. F. Gantmakher, M. V. Golubkov, V. T. Dolgopolov, G. E. Tsydynzhapov, and A. A. Shashkin, Jetp Letters **68**, 363 (1998).